JOURNAL OF MOLECULAR SPECTROSCOPY **180,** 402–413 (1996)
ARTICLE NO. 0264

The Rotational Spectrum of H_2Te

Igor N. Kozin,*[,1] Per Jensen,* Oliver Polanz,† Stefan Klee,‡ Laurent Poteau,§ and Jean Demaison§

*Fachbereich 9, Theoretische Chemie, Bergische Universität–Gesamthochschule Wuppertal, D-42097 Wuppertal, Germany; †Fachbereich 9, Anorganische Chemie, Bergische Universität–Gesamthochschule Wuppertal, D-42097 Wuppertal, Germany; ‡Physikalisch-Chemisches Institut, Justus-Liebig-Universität, Heinrich-Buff-Ring 58, D-35392 Giessen, Germany; and §Laboratoire de Spectroscopie Hertzienne, URA CNRS 249, Bâtiment P5, Université de Lille I, F-59655 Villeneuve d'Ascq, France

Received May 14, 1996; in revised form July 1, 1996

In the present work, we study the spectrum of the H_2Te molecule in the submillimeter-wave and far infrared region. An important aim of this investigation is the further experimental characterization of the anomalous ''four-fold cluster effect'' exhibited by the rotational energy levels in the vibrational ground state of H_2Te. The spectrum in the region 90–472 GHz was measured with a source-modulated millimeter-wave spectrometer and that between 600 and 1600 GHz with a far-infrared sideband spectrometer. The far infrared spectrum from 30 to 360 cm^{-1} was measured with a Bruker IFS 120 HR interferometer attached to a 3 m long cell. We have assigned 224 submillimeter-wave lines and 1695 FIR lines. These observed data were supplemented by a large number of ground state combination differences derived from rotation–vibration bands of H_2Te, and the resulting large data set was analyzed by means of a modified Watson Hamiltonian. Accurate sets of rotational and centrifugal distortion constants for all eight tellurium isotopomers were obtained.

I. INTRODUCTION

We report here an experimental study of the rotational spectrum of H_2Te, based on far infrared spectra, obtained with Fourier transform infrared spectrometers, and submillimeter-wave spectra obtained with a millimeter-wave spectrometer or a laser sideband system. One of the principal aims of the present work is to characterize further the so-called fourfold energy clusters formed by the rotational energies of H_2X molecules, X = S, Se, and Te (see Ref. (*1*) and references therein). The existence of these four-member groups of nearly degenerate energy levels at high rotational excitation has been experimentally verified for the vibrational ground state (*2–4*) and for the ν_1/ν_3 vibrational states (*5*) of H_2Se and, very recently, some indication of cluster formation was observed in H_2S.[2]

Prior to its experimental verification, the cluster effect in H_2X molecules was predicted by means of classical and semiclassical methods (*6–9*). More recently, it has been theoretically investigated by realistic quantum mechanical calculations carried out with the MORBID (Morse oscillator rigid bender internal dynamics) Hamiltonian and computer program (*10, 11*) for H_2S (*12*), H_2Se (*13, 14*), and H_2Te (*1, 15, 16*).

The previous theoretical studies of the cluster effect in H_2Te were based on an *ab initio* potential energy surface (*15*) and on a surface (*1, 16*) obtained in a least-squares fit (using the MORBID program) to experimental term values involving $J \leqslant 5$ from Refs. (*17–23*). The calculations showed that the cluster formation in H_2Te is highly similar to that in H_2Se, and they stimulated new experimental work on H_2Te aimed at further characterization of the cluster effect. In parallel to the study of the rotational spectrum reported in the present work, analyses of newly recorded Fourier transform infrared spectra of H_2Te are being carried out. They involve the ν_2 band (*24*) and the stretching fundamental transitions together with several overtone and combination bands (*25*). An important objective of the present work is to facilitate these analyses by providing accurate molecular parameters for the vibrational ground state of H_2Te.

The theoretical calculations of the rotational energy level structures in the vibrational ground states of H_2S (*12*) and H_2Se (*13, 14*) showed that in H_2Se, the clusters form at lower J values than in H_2S. Hence it was initially surmised that in H_2Te, clusters would form at lower J values than in H_2Se, so that they would be easily amenable to experimental observation. However, *ab initio* calculations for H_2Te (*15*) showed that even though classical and semi-classical calcu-

[1] On leave from Applied Physics Institute, Russian Academy of Science, Uljanov Street 47, Nizhnii Novgorod 603600, Russia.

[2] O. L. Polyansky, S. Klee, G. Ch. Mellau, J. Demaison, and P. Jensen, Poster B17, Fourteenth Colloquium on High Resolution Molecular Spectroscopy, Dijon, France, September 1995; L. R. Brown, J. Crisp, D. Crisp, A. Bykov, O. Naumenko, M. Smirnov, L. Sinitsa, and A. Perrin, Poster F14, Fourteenth Colloquium on High Resolution Molecular Spectroscopy, Dijon, France, September 1995.

0022-2852/96 $18.00

lations had predicted the so-called critical J value, J_c, for H_2Te to be lower than that for H_2Se, the clusters form at comparative J values in the two molecules. At $J = J_c$, the energy difference between the highest two doublets in each J manifold starts decreasing with J, and the cluster formation becomes evident. The fact that relative to H_2Se, the clusters do not appear at significantly lower J values in H_2Te, can be thought of as a simple consequence of the ''quantum nature'' of the rotational motion at low J. This motion is not well described by the classical or semi-classical methods used to estimate J_c. A further problem with the observation of cluster states in H_2Te is the fact that H_2Te thermally decomposes into H_2 molecules and solid Te. This makes it impossible to heat the H_2Te sample during the experiment to populate the high-J cluster states. In fact, during the experiments reported in the present work, it was necessary to cool the cell to temperatures below -30°C.

Prior to the present work, the only direct source of experimental data characterizing the vibrational ground state of H_2Te was the submillimeter-wave spectrum recorded by Burenin *et al.* (*23*). We supplement these data with transition wavenumbers obtained from Fourier transform far infrared spectra, with submillimeter-wave transition frequencies recorded with a millimeter-wave spectrometer or a laser sideband system, and with ground state combination differences from rotation–vibration bands recorded with Fourier transform infrared interferometers (*24, 25*), and carry out a simultaneous analysis of the combined data set by means of a modified Watson-type effective Hamiltonian. We have succeeded in observing a few transitions between energy levels in the fourfold cluster region. Even though the observed levels form clusters as predicted theoretically (*1, 15, 16*), the ''cluster rate'' (i.e., the decrease with J of the energy differences between the individual energies forming a cluster) is not as high as found for H_2Se (*13, 14*).

II. EXPERIMENTAL DETAILS

(a) Synthesis

As the first step in the synthesis of hydrogen telluride (*26*), elementary tellurium was heated to 500°C together with elementary aluminum to form Al_2Te_3, which was treated with HCl to produce H_2Te. The H_2Te was separated from the HCl remaining in the reaction vessel by means of fractional condensation *in vacuo*, the H_2Te condensing in a trap held at -140°C, whereas the residual HCl was condensed in another trap at -196°C. The sample contained the tellurium isotopes ^{130}Te (0.3380), ^{128}Te (0.3169), ^{126}Te (0.1895), ^{125}Te (0.0714), ^{124}Te (0.0482), ^{123}Te (0.0091), ^{122}Te (0.0260), and ^{120}Te (0.0009) in natural abundance. The numbers in parentheses are the natural abundances (*27*) for each isotope.

(b) Fourier Transform Infrared Spectra

High resolution Fourier transform spectra in the far infrared spectral region were measured with the BRUKER IFS 120 HR interferometer at the Justus Liebig University Giessen. In order to allow the observation of weak transitions involving the highly excited rotational states of primary interest in the present study, an optimum signal-to-noise level had to be achieved. Therefore, the far infrared region was divided into two sections (20–100 and 90–370 cm^{-1}, respectively), both being recorded separately with appropriate optical and electronic filters, beamsplitters, and aperture diameters. In both cases a mercury lamp served as radiation source and a silicon bolometer operating at 4.2 K as detector.

Since hydrogen telluride decomposes thermally, the available measurement time is strongly limited at ambient temperature. Therefore, the spectroscopic experiments were carried out within the temperature range 230–250 K using a home-built variable-temperature absorption cell having an optical pathlength of 302 cm (*28*). Furthermore, to prevent photodecomposition of the sample, its transfer from the storage bulb into the absorption cell through a glass vacuum line was performed in a darkened room. The initial H_2Te pressures in the cell for the two runs were 280 and 500 Pa, respectively. In spite of the precautions, a substantial precipitation of tellurium on the glass walls was observed. From an analysis of the decreasing spectral line absorbance during the two runs we determined the effective pressure to be 246 and 418 Pa, respectively (*29*).

Spectra were recorded at an unapodized resolution (MOPD^{-1}) of 0.0018 cm^{-1}. Each spectrum consisted of up to 220 individual scans that were coadded and ratioed against the spectrum of the empty cell. For calibration we determined the positions of some water rotational lines occurring in the spectra. These transition wavenumbers, together with their literature values (*30*), were used to calculate a calibration constant in a linear regression procedure. The standard deviation of the calibrated measured line positions from their literature values was determined to be about 5×10^{-5} cm^{-1}.

Figure 1 shows a small part of the Fourier transform far infrared spectrum. Owing to the many tellurium isotopes with significant abundances (see above), the spectrum consists of characteristic groups of lines with a common assignment but belonging to different H_2Te isotopomers. One such group, where each line is assigned as the unresolved transition doublet $J_{K_a;K_c} = 10_{4;7} \leftarrow 9_{1;8}$ and $10_{3;7} \leftarrow 9_{2;8}$, is seen in the figure. The spectrum has many relatively strong H_2S impurity lines, and one of these transitions is seen in the central part of the figure. On the right hand side of Fig. 1 we find another group of H_2Te lines whose members are assigned as the weak ''cluster transition'' $J_{K_aK_c} = 14_{14;0} \leftarrow 13_{13;1}$.

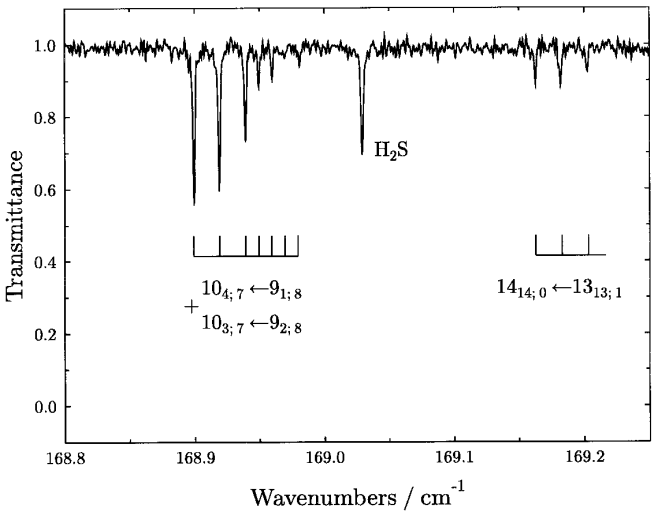

FIG. 1. A section of the FIR H_2Te absorption spectrum recorded at an effective pressure of 418 Pa.

(c) Submillimeter-wave Spectra

In Lille, the rotational spectrum was measured with two different spectrometers. Between 90 and 472 GHz a source-modulated spectrometer was used. The radiation source is either phase-locked submillimeter-wave backward-wave oscillators (Thomson-CSF) (340–472 GHz) or, below 340 GHz, a GaAs Schottky multiplier driven by phase-locked klystrons. A He-cooled bolometer is used for the detection. The estimated accuracy of the measurements is about 30–50 kHz, depending on the signal/noise ratio. The submillimeter-wave spectrum was measured between 600 and 1600 GHz with a far infrared microwave sideband spectrometer described in Ref. (*31*). The outputs of a computer controlled synthesizer (2–18 GHz) and an optically pumped far infrared laser are mixed on a Schottky diode in order to generate the sum and difference frequencies. The tunability of the sideband radiation is ±18 GHz around each laser frequency. A heterodyne receiver is used to detect the sideband signal, with the unmodulated part of the primary laser power being used as a local oscillator. The accuracy of the frequency measurements depends mainly on the accuracy of the frequency of the laser line. Below 1 THz it is generally about 500 kHz and 1 MHz above. Most measurements were made at −30°C with a sample pressure around 2×10^{-2} mbar. Under these conditions the lifetime of H_2Te allows measurements for about 30 min. The high-K lines were measured at room temperature, which necessitated a refilling of the cell after each measurement. The millimeter-wave and submillimeter-wave spectra were measured in parallel with the assignment of the far-infrared spectrum. Thus, the first frequency prediction was calculated with the parameters obtained from fitting the FIR lines. The intensities of the rotational lines were estimated using an *ab initio* dipole moment function (*29*).

III. ANALYSIS

As a preliminary step in the analysis of the data we obtained an initial set of rotation–vibration parameters for the vibrational ground state by fitting the known submillimeter-wave frequencies (*23*) and the ground state combination differences from $\nu_1 + \nu_2$ and $\nu_2 + \nu_3$ bands (*20*) separately for each H_2Te isotopomer. In the present work, we could include most of the submillimeter-wave lines from Ref. (*23*) in the input data for the fitting. In Ref. (*23*), only a very small part of these lines were fitted, presumably because of difficulties in finding an appropriate model. In the fits, each data point was assigned a weight factor of $1/\delta_i^2$, where δ_i is the estimated uncertainty of the measured frequency or wavenumber. The uncertainties of the submillimeter-wave data of Ref. (*23*) are estimated to be 100 kHz for transitions of the isotopomers of $H_2^{130}Te$, $H_2^{128}Te$, and $H_2^{126}Te$ and 200 kHz for transitions belonging to the remaining isotopomers. The initial analysis showed that several of the submillimeter-wave lines from Ref. (*23*) had residuals (observed − calculated) significantly larger than their estimated uncertainties. We have discarded all transitions whose residuals exceed three times the corresponding estimated uncertainty. We believe that for these transitions, the frequency values predicted from the parameters obtained in the initial fitting will be more accurate than the experimental values from Ref. (*23*).

In the next step of the analysis, we used the initial parameter set, together with the dipole moment parameters from Ref. (*29*), to simulate the frequencies/wavenumbers and the intensities of the H_2Te rotational spectrum. We could now proceed in a bootstrap manner to analyze the complete Fourier transform far infrared spectrum. In parallel with this analysis, the submillimeter-wave spectrum of H_2Te was measured (see Section II). These measurements were supported by predictions obtained with the successively improved molecular parameters determined in the bootstrap procedure. The procedure was essentially the same as we used for H_2Se (*4*). Generally the uncertainties of the far infrared data was set to 0.0001 cm^{-1}. The accuracy of the submillimeter-wave lines varies from 50 kHz to 1 MHz depending on the frequency region (see Table 1).

The fits were made with a modified Watson Hamiltonian (*2*),

$$H = \frac{1}{2}(B + C)\hat{J}^2 + \left(A - \frac{1}{2}(B + C)\right)\hat{J}_z^2 + \sum_{ij} c_{ij}(\hat{J}^2 - \hat{J}_z^2)^i(\hat{J}_z^2)^j + \frac{1}{2}\left[\left\{\frac{1}{4}(B - C) + \sum_{ij} b_{ij}(\hat{J}^2 - \hat{J}_z^2)^i(\hat{J}_z^2)^j\right\}, \{\hat{J}_+^2 + \hat{J}_-^2\}\right]_+, \quad [1]$$

TABLE 1

Microwave Rotational Transitions in the Vibrational Ground State of H_2Te

obs.	o.–c.	J'	K_a'	K_c'	J''	K_a''	K_c''	unc.	obs.	o.–c.	J'	K_a'	K_c'	J''	K_a''	K_c''	unc.
			$H_2{}^{130}Te$						656525.63	−0.025	4	1	3	4	0	4	0.5
96314.531	0.023	1	1	0	1	0	1	0.05	656672.97	0.164	4	2	3	4	1	4	0.5
100943.355	0.114	2	2	0	2	1	1	0.05	994554.08	0.736	12	7	5	12	6	6	0.5
147208.975	−0.061	6	6	0	6	5	1	0.05	996553.02	0.007	12	8	5	12	7	6	0.5
228615.226	0.000	10	10	0	10	9	1	0.05	1003354.33	0.654	5	0	5	4	1	4	1.
250478.07[a]	−0.027	7	6	1	7	5	2	0.1	1003356.20	0.622	5	1	5	4	0	4	1.
251571.51[a]	0.094	6	5	1	6	4	2	0.1	1009544.57	1.141	10	5	5	10	4	6	1.
254292.44[a]	0.059	8	7	1	8	6	2	0.1	1009975.19	0.849	4	2	3	3	1	2	1.
256023.16[a]	0.002	5	4	1	5	3	2	0.1	1184996.94	0.382	6	1	6	5	0	5	1.
262334.95[a]	0.162	4	3	1	4	2	2	0.1		0.532	6	0	6	5	1	5	
269139.58[a]	−0.273	3	2	1	3	1	2	0.1	1190164.07	−0.360	11	5	6	11	4	7	1.
275283.47[a]	0.272	2	1	1	2	0	2	0.1	1190239.98	0.160	11	6	6	11	5	7	1.
278315.13[a]	0.034	1	1	1	0	0	0	0.1	1190370.77	−0.440	5	1	4	4	2	3	1.
288657.85[a,b]	0.437	2	2	1	2	1	2	0.1	1190534.97	−0.889	5	2	4	4	1	3	1.
294682.89[a]	0.244	3	3	1	3	2	2	0.1	1196553.38	0.681	3	3	0	2	2	1	1.
302208.048	−0.054	4	4	1	4	3	2	0.05	1197835.28	−0.285	10	4	6	10	3	7	1.
310090.717	−0.006	11	10	1	11	9	2	0.05	1197859.10	0.415	10	5	6	10	4	7	1.
310758.083	−0.008	5	5	1	5	4	2	0.05	1378934.34	−0.468	11	4	7	11	3	8	1.
319701.92[a,b]	−1.098	6	6	1	6	5	2	0.1	1378937.92	−0.590	11	5	7	11	4	8	1.
328257.42[a]	0.117	7	7	1	7	6	2	0.1	1380117.61	−0.369	5	3	3	4	2	2	1.
335493.85[a]	0.113	8	8	1	8	7	2	0.1	1387723.86	0.078	10	4	7	10	3	8	1.
340378.274	0.032	9	9	1	9	8	2	0.05		0.940	10	3	7	10	2	8	
341826.728	−0.027	10	10	1	10	9	2	0.05	1403314.71	0.728	8	2	7	8	1	8	1.
347593.568	0.063	12	11	1	12	10	2	0.05		0.749	8	1	7	8	0	8	
376367.092	0.013	13	11	2	13	10	3	0.05	1547682.09	0.360	13	5	8	13	4	9	1.
377838.236	−0.019	12	10	2	12	9	3	0.05	1547684.69	−0.133	13	6	8	13	5	9	1.
383238.962	0.006	14	12	2	14	11	3	0.05	1547913.52	0.684	8	1	8	7	0	7	1.
386083.293	0.051	11	9	2	11	8	3	0.05		0.686	8	0	8	7	1	7	
395591.183	−0.064	13	12	1	13	11	2	0.05	1557607.31	0.454	6	2	4	5	3	3	1.
398841.817	−0.084	10	8	2	10	7	3	0.05	1558274.35	0.743	6	3	4	5	2	3	1.
413689.36[a]	0.136	9	7	2	9	6	3	0.1	1559005.81	0.990	4	4	0	3	3	1	1.
428474.49[a]	0.192	8	6	2	8	5	3	0.1	1559074.43	−1.322	12	4	8	12	3	9	1.
441612.141	0.002	7	5	2	7	4	3	0.05	1559077.42	0.892	12	5	8	12	4	9	1.
452201.013	−0.044	6	4	2	6	3	3	0.05				$H_2{}^{128}Te$					
453837.286	0.029	14	13	1	14	12	2	0.05	96348.599	0.013	1	1	0	1	0	1	0.05
455382.298	−0.021	2	0	2	1	1	1	0.05	101025.142	0.020	2	2	0	2	1	1	0.05
459981.907	−0.066	5	3	2	5	2	3	0.05	147830.927	−0.037	6	6	0	6	5	1	0.05
460333.362	0.013	2	1	2	1	0	1	0.05	230260.156	−0.016	10	10	0	10	9	1	0.05
465184.996	−0.043	4	2	2	4	1	3	0.05	250318.01[a]	−0.009	7	6	1	7	5	2	0.1
468325.707	0.027	3	1	2	3	0	3	0.05	251386.22[a]	0.320	6	5	1	6	4	2	0.1
470093.228	0.007	3	2	2	3	1	3	0.05	254205.50[a]	0.002	8	7	1	8	6	2	0.1
470349.681	0.002	4	3	2	4	2	3	0.05	255851.06[a]	0.068	5	4	1	5	3	2	0.1
471605.415	−0.074	5	4	2	5	3	3	0.05	262202.49[a]	0.119	4	3	1	4	2	2	0.1
474364.71[a]	−0.004	6	5	2	6	4	3	0.1	269059.68[a]	−0.035	3	2	1	3	1	2	0.1
479136.42[a]	0.010	7	6	2	7	5	3	0.1	275254.97[a]	0.209	2	1	1	2	0	2	0.1
486409.78[a]	−0.036	8	7	2	8	6	3	0.1	278370.69[a]	0.210	1	1	1	0	0	0	0.1
620469.89	0.495	10	7	3	10	6	4	0.5	288759.75[a]	0.253	2	2	1	2	1	2	0.1
631997.24	0.432	9	6	3	9	5	4	0.5	294853.33[a]	0.263	3	3	1	3	2	2	0.1
639610.10	0.282	3	0	3	2	1	2	0.5	302469.788	−0.031	4	4	1	4	3	2	0.05
639991.70	0.400	3	1	3	2	0	2	0.5	310518.613	−0.021	11	10	1	11	9	2	0.05
640492.37	0.372	8	5	3	8	4	4	0.5	311133.475	−0.015	5	5	1	5	4	2	0.05
646616.60	0.002	7	4	3	7	3	4	0.5	320213.13[a]	0.101	6	6	1	6	5	2	0.1
647709.13	0.037	10	8	3	10	7	4	0.5	328920.38[a]	0.120	7	7	1	7	6	2	0.1
647791.40	0.056	9	7	3	9	6	4	0.5	336324.18[a]	0.074	8	8	1	8	7	2	0.1
648874.57	−0.182	8	6	3	8	5	4	0.5	340146.199	0.031	11	11	1	11	10	2	0.05
648898.25	−0.221	11	9	3	11	8	4	0.5	341385.382	0.039	9	9	1	9	8	2	0.05
650616.76	−0.066	7	5	3	7	4	4	0.5	343013.544	−0.009	10	10	1	10	9	2	0.05
651012.28	0.089	6	3	3	6	2	4	0.5	348249.347	0.070	12	11	1	12	10	2	0.05
652676.61	0.356	2	2	1	1	1	0	0.5	376627.380	−0.038	13	11	2	13	10	3	0.05
652677.48	0.132	6	4	3	6	3	4	0.5	377802.731	0.016	12	10	2	12	9	3	0.05

Note: Observed transition frequencies, residuals (observed — calculated) and uncertainties are given in MHz.
[a] From Ref. *(23)*. [b] Line excluded from the fitting.

where $\hat{J}_x$, $\hat{J}_y$, and $\hat{J}_z$ are the components of the total angular momentum along the molecule-fixed axes, $\hat{J}^2 = \hat{J}_x^2 + \hat{J}_y^2 + \hat{J}_z^2$, $\hat{J}_\pm = \hat{J}_x \pm i\hat{J}_y$, and the plus commutator of two operators $\hat{A}$ and $\hat{B}$ is $[\hat{A}, \hat{B}]_+ = \hat{A}\hat{B} + \hat{B}\hat{A}$. The effective Hamiltonian of Eq. [1] is simply a reparameterization of the standard Watson Hamiltonian in A reduction and I^r representation. If all parameters are fitted up to a given order of perturbation theory, the Hamiltonian of Eq. [1] will produce a fit identical to that obtained with the standard Watson Hamiltonian. However, as discussed below, the parameter values obtained with the modified Hamiltonian are generally less correlated than those obtained with the standard Watsonian. For ''rare'' isotopomers with relatively few observed transitions, poorly defined parameters were constrained to the values obtained for more abundant isotopomers.

In the final step of the analysis, a large data set of ground

TABLE 1—*Continued*

obs.	o.–c.	J'	K_a'	K_c'	J''	K_a''	K_c''	unc	obs.	o.–c.	J'	K_a'	K_c'	J''	K_a''	K_c''	unc.
383912.955	0.012	14	12	2	14	11	3	0.05	1558462.96	0.703	6	3	4	5	2	3	1.
385869.321	0.053	11	9	2	11	8	3	0.05	1559107.40	0.738	4	4	0	3	3	1	1.
396447.858	−0.010	13	12	1	13	11	2	0.05	1559249.57	0.010	12	5	8	12	4	9	1.
398553.249	−0.101	10	8	2	10	7	3	0.05				$H_2{}^{126}Te$					
413405.91[a]	0.089	9	7	2	9	6	3	0.1	96383.792	0.066	1	1	0	1	0	1	0.05
428246.11[a]	0.034	8	6	2	8	5	3	0.1	101109.597	−0.024	2	2	0	2	1	1	0.05
441460.215	−0.008	7	5	2	7	4	3	0.05	148473.715	−0.055	6	6	0	6	5	1	0.05
452123.861	−0.015	6	4	2	6	3	3	0.05	231958.803	0.001	10	10	0	10	9	1	0.05
454816.976	0.046	14	13	1	14	12	2	0.05	250156.54[a]	−0.092	7	6	1	7	5	2	0.1
455411.007	−0.034	2	0	2	1	1	1	0.05	251196.88[a]	0.057	6	5	1	6	4	2	0.1
459964.350	−0.041	5	3	2	5	2	3	0.05	254121.72[a]	0.283	8	7	1	8	6	2	0.1
460410.032	0.000	2	1	2	1	0	1	0.05	255674.67[a]	0.043	5	4	1	5	3	2	0.1
465207.310	−0.047	4	2	2	4	1	3	0.05	262066.53[a]	0.216	4	3	1	4	2	2	0.1
468370.138	−0.038	3	1	2	3	0	3	0.05	268976.94[a]	−0.254	3	2	1	3	1	2	0.1
470153.801	−0.011	3	2	2	3	1	3	0.05	275225.82[a,b]	0.428	2	1	1	2	0	2	0.1
470418.333	−0.004	4	3	2	4	2	3	0.05	278428.21[a,b]	0.639	1	1	1	0	0	0	0.1
471689.519	−0.036	5	4	2	5	3	3	0.05	288864.96[a]	0.196	2	2	1	2	1	2	0.1
474473.51[a]	−0.024	6	5	2	6	4	3	0.1	295029.43[a,b]	0.562	3	3	1	3	2	2	0.1
479280.37[a]	0.010	7	6	2	7	5	3	0.1	302739.815	−0.019	4	4	1	4	3	2	0.05
486598.73[a]	−0.055	8	7	2	8	6	3	0.1	310971.539	0.000	11	10	1	11	9	2	0.05
631899.05	0.147	9	6	3	9	5	4	0.5	311520.808	0.000	5	5	1	5	4	2	0.05
639683.30	0.108	3	0	3	2	1	2	0.5	320739.31[a]	0.065	6	6	1	6	5	2	0.1
640068.60	0.334	3	1	3	2	0	2	0.5	329604.52[a]	0.218	7	7	1	7	6	2	0.1
640468.09	−0.908	8	5	3	8	4	4	0.5	337180.94[a]	0.038	8	8	1	8	7	2	0.1
646641.24	−0.012	7	4	3	7	3	4	0.5	413112.01[a]	−0.052	9	7	2	9	6	3	0.1
647865.07	−0.428	10	8	3	10	7	4	0.5	428008.90[a]	0.016	8	6	2	8	5	3	0.1
647905.29	−0.053	9	7	3	9	6	4	0.5	441301.963	0.013	7	5	2	7	4	3	0.05
648964.81	0.045	8	6	3	8	5	4	0.5	452043.120	−0.025	6	4	2	6	3	3	0.05
650695.25	−0.189	7	5	3	7	4	4	0.5	455440.567	−0.005	2	0	2	1	1	1	0.05
651064.77	0.082	6	3	3	6	2	4	0.5	459945.565	−0.014	5	3	2	5	2	3	0.05
652752.12	−0.142	6	4	3	6	3	4	0.5	460489.109	0.024	2	1	2	1	0	1	0.05
652821.07	0.128	2	2	1	1	1	0	0.5	465229.988	−0.025	4	2	2	4	1	3	0.05
656600.21	−0.344	4	1	3	4	0	4	0.5	468415.848	−0.012	3	1	2	3	0	3	0.05
656749.58	−0.092	4	2	3	4	1	4	0.5	470216.298	0.037	3	2	2	3	1	3	0.05
994608.84	0.770	12	7	5	12	6	6	1.	470489.240	−0.006	4	3	2	4	2	3	0.05
996638.14	0.281	12	8	5	12	7	6	1.	471776.520	−0.041	5	4	2	5	3	3	0.05
1003472.17	1.038	5	0	5	4	1	4	1.	474586.370	0.008	6	5	2	6	4	3	0.1
1003474.15	1.094	5	1	5	4	0	4	1.	479429.840	0.015	7	6	2	7	5	3	0.1
1009986.42	0.879	10	6	5	10	5	6	1.	486795.150	−0.063	8	7	2	8	6	3	0.1
1009639.12	0.815	10	5	5	10	4	6	1.	1190410.260	−0.569	11	5	6	11	4	7	1.
1185135.09	−0.088	6	1	6	5	0	5	1.				$H_2{}^{125}Te$					
1190285.63	−0.250	11	5	6	11	4	7	1.	96401.718	0.059	1	1	0	1	0	1	0.05
1190361.96	−0.201	11	6	6	11	5	7	1.	101152.640	−0.093	2	2	0	2	1	1	0.05
1190509.43	−0.742	5	1	4	4	2	3	1.	148802.039	−0.106	6	6	0	6	5	1	0.05
1190677.25	0.269	5	2	4	4	1	3	1.	232826.438	0.022	10	10	0	10	9	1	0.05
1196647.66	0.083	3	3	0	2	2	1	1.	250075.65[a]	0.173	7	6	1	7	5	2	0.2
1197964.82	0.268	10	4	6	10	3	7	1.	251101.06[a]	−0.110	6	5	1	6	4	2	0.2
1197988.14	0.195	10	5	6	10	4	7	1.	254080.50[a]	0.338	8	7	1	8	6	2	0.2
1379085.89	−0.230	11	4	7	11	3	8	1.	255585.02[a]	−0.125	5	4	1	5	3	2	0.2
1379089.46	−0.419	11	5	7	11	4	8	1.	261997.37[a]	0.207	4	3	1	4	2	2	0.2
1380311.50	−0.459	5	3	3	4	2	2	1.	275211.02[a]	0.556	2	1	1	2	0	2	0.2
1387880.05	−0.257	10	4	7	10	3	8	1.	278457.30[a]	0.614	1	1	1	0	0	0	0.2
	0.617	10	3	7	10	2	8		288918.64[a]	0.161	2	2	1	2	1	2	0.2
1403479.14	0.094	8	2	7	8	1	8	1.	295118.89[a]	0.354	3	3	1	3	2	2	0.2
	0.115	8	1	7	8	0	8		302877.539	−0.011	4	4	1	4	3	2	0.05
1547847.91	−0.491	13	5	8	13	4	9	1.	311718.479	0.071	5	5	1	5	4	2	0.05
1547850.65	−0.887	13	6	8	13	5	9	1.	321008.26[a]	0.409	6	6	1	6	5	2	0.2
1548094.14	0.406	8	1	8	7	0	7	1.	329954.18[a]	0.491	7	7	1	7	6	2	0.2
	0.408	8	0	8	7	1	7		337618.83[a]	0.087	8	8	1	8	7	2	0.2
1557787.33	0.550	6	2	4	5	3	3	1.	412961.15[a]	0.068	9	7	2	9	6	3	0.2

state combination differences from the ν_2 (*24*) and the ν_1/ν_3 bands (*25*) was added to the input data for the fitting. In the final fit, the input data sets for the various isotopomers consisted of submillimeter-wave lines from Ref. (*23*), newly measured submillimeter-wave lines (see Section II), newly measured Fourier transform far infrared lines, and ground state combination differences from Refs. (*24, 25*). The uncertainties for the submillimeter-wave lines and the Fourier transform infrared lines are described above, and the uncertainties δ_i for the combination differences were set to the sum of the uncertainties for the two transitions (this sum is about 0.0004 cm^{-1}). Table 1 gives the complete set of all submillimeter-wave rotational transitions in the vibrational ground states of all isotopomers of H_2Te, and Table 2 gives the measured Fourier transform far infrared transitions measured for $H_2{}^{130}Te$. The complete input data sets for the final fittings are available from the authors on request. The statistics of the final fittings are compiled in Table 3 together with the parameter values obtained. The dimensionless standard deviations in Table 3 are calculated separately for the submillimeter-wave lines, the FIR lines, and the ground state combination differences. They are defined as

TABLE 1—*Continued*

obs.	o.–c.	J'	K_a'	K_c'	J''	K_a''	K_c''	unc.
427887.09[a]	−0.007	8	6	2	8	5	3	0.2
441220.640	0.013	7	5	2	7	4	3	0.05
452001.421	−0.117	6	4	2	6	3	3	0.05
455455.556	−0.067	2	0	2	1	1	1	0.05
459935.714	0.000	5	3	2	5	2	3	0.05
460529.447	0.035	2	1	2	1	0	1	0.05
465241.464	0.018	4	2	2	4	1	3	0.05
468439.169	0.009	3	1	2	3	0	3	0.05
470248.116	−0.079	3	2	2	3	1	3	0.05
470525.533	0.032	4	3	2	4	2	3	0.05
471821.076	−0.000	5	4	2	5	3	3	0.05
474644.09[a]	−0.072	6	5	2	6	4	3	0.2
479506.55[a]	0.020	7	6	2	7	5	3	0.2
486896.13[a]	−0.136	8	7	2	8	6	3	0.2
			$H_2{}^{124}Te$					
96419.925	−0.081	1	1	0	1	0	1	0.05
101196.873	0.002	2	2	0	2	1	1	0.05
149138.432	−0.031	6	6	0	6	5	1	0.05
233713.615	−0.021	10	10	0	10	9	1	0.05
249994.04[a]	0.267	7	6	1	7	5	2	0.2
251004.16[a]	0.155	6	5	1	6	4	2	0.2
254040.23[a]	0.116	8	7	1	8	6	2	0.2
255494.08[a]	0.175	5	4	1	5	3	2	0.2
261926.78[a]	0.263	4	3	1	4	2	2	0.2
275195.90[a,b]	0.749	2	1	1	2	0	2	0.2
278487.12[a]	0.602	1	1	1	0	0	0	0.2
288973.85[a]	0.419	2	2	1	2	1	2	0.2
295210.54[a]	0.213	3	3	1	3	2	2	0.2
303018.462	−0.061	4	4	1	4	3	2	0.05
311451.013	0.009	11	10	1	11	9	2	0.05
311920.660	0.080	5	5	1	5	4	2	0.05
321282.45[a]	−0.001	6	6	1	6	5	2	0.20
330310.85[a]	0.285	7	7	1	7	6	2	0.2
338065.58[a]	−0.125	8	8	1	8	7	2	0.2
412807.28[a]	0.066	9	7	2	9	6	3	0.2
427762.25[a]	0.101	8	6	2	8	5	3	0.2
441136.896	0.010	7	5	2	7	4	3	0.05
451958.518	−0.062	6	4	2	6	3	3	0.05
455471.037	−0.015	2	0	2	1	1	1	0.05
459925.423	0.002	5	3	2	5	2	3	0.05
460570.696	−0.021	2	1	2	1	0	1	0.05
465253.048	0.006	4	2	2	4	1	3	0.05
468462.902	0.016	3	1	2	3	0	3	0.05
470280.817	0.043	3	2	2	3	1	3	0.05
470562.523	−0.052	4	3	2	4	2	3	0.05
471866.587	−0.054	5	4	2	5	3	3	0.05
474702.62[a,b]	−0.688	6	5	2	6	4	3	0.2
479585.06[a]	0.126	7	6	2	7	5	3	0.2
486999.43[a]	0.054	8	7	2	8	6	3	0.2
			$H_2{}^{123}Te$					
149479.212	−0.006	6	6	0	6	5	1	0.05
249912.39[a]	0.115	7	6	1	7	5	2	0.2
255402.13[a,b]	0.900	5	4	1	5	3	2	0.2
303160.65[a,b]	−1.161	4	4	1	4	3	2	0.2
311706.178	−0.015	11	10	1	11	9	2	0.05
312126.144	0.019	5	5	1	5	4	2	0.05
321560.85[a]	−0.050	6	6	1	6	5	2	0.2
338537.70[a,b]	25.681	8	8	1	8	7	2	0.2
412650.77[a]	−0.027	9	7	2	9	6	3	0.2
441051.912	0.007	7	5	2	7	4	3	0.05
451914.891	0.001	6	4	2	6	3	3	0.05
455486.551	0.034	2	0	2	1	1	1	0.05
459914.845	−0.015	5	3	2	5	2	3	0.05
460612.335	−0.034	2	1	2	1	0	1	0.05
465264.699	−0.005	4	2	2	4	1	3	0.05
468486.884	0.003	3	1	2	3	0	3	0.05
470313.676	−0.019	3	2	2	3	1	3	0.05
470600.091	0.056	4	3	2	4	2	3	0.05
471912.787	−0.040	5	4	2	5	3	3	0.05
474762.51[a,b]	−1.033	6	5	2	6	4	3	0.2
479665.05[a]	0.025	7	6	2	7	5	3	0.2
487104.54[a]	−0.043	8	7	2	8	6	3	0.2
			$H_2{}^{122}Te$					
96457.454	0.020	1	1	0	1	0	1	0.05
101286.988	0.049	2	2	0	2	1	1	0.05
149826.137	0.010	6	6	0	6	5	1	0.05
235527.277	0.013	10	10	0	10	9	1	0.05
249829.81[a]	−0.083	7	6	1	7	5	2	0.2
250807.67[a]	0.162	6	5	1	6	4	2	0.2
253962.50[a]	0.130	8	7	1	8	6	2	0.2
255308.70[a]	0.034	5	4	1	5	3	2	0.2
261782.93[a]	0.144	4	3	1	4	2	2	0.2
295397.88[a]	0.206	3	3	1	3	2	2	0.2
303306.353	0.000	4	4	1	4	3	2	0.05
312333.470	−0.044	5	5	1	5	4	2	0.05
321843.80[a]	0.337	6	6	1	6	5	2	0.2
427505.67[a]	0.210	8	6	2	8	5	3	0.2
440964.730	−0.026	7	5	2	7	4	3	0.05
451870.031	0.008	6	4	2	6	3	3	0.05
455502.479	0.018	2	0	2	1	1	1	0.05
459903.895	0.023	5	3	2	5	2	3	0.05
460654.904	−0.013	2	1	2	1	0	1	0.05
465276.486	0.013	4	2	2	4	1	3	0.05
468511.275	−0.040	3	1	2	3	0	3	0.05
470347.432	0.035	3	2	2	3	1	3	0.05
470638.351	−0.039	4	3	2	4	2	3	0.05
471959.955	−0.002	5	4	2	5	3	3	0.05
474824.56[a]	−0.163	6	5	2	6	4	3	0.2
479746.40[a]	0.143	7	6	2	7	5	3	0.2
487212.01[a]	0.049	8	7	2	8	6	3	0.2
			$H_2{}^{120}Te$					
440796.647	−0.001	7	5	2	7	4	3	0.05
460741.711	0.028	2	1	2	1	0	1	0.05
470716.831	−0.010	4	3	2	4	2	3	0.05

$$\sigma_S = \sqrt{\frac{1}{N_S}\sum_i \left(\frac{\nu_i^{(\mathrm{obs})} - \nu_i^{(\mathrm{calc})}}{\delta_i}\right)^2}, \qquad [2]$$

where N_S is the number of input data of a given type (i.e., submillimeter-wave lines, FIR lines, or ground state combination differences), the sum runs over these input data, and $\nu_i^{(\mathrm{obs})}$ and $\nu_i^{(\mathrm{calc})}$ are observed and calculated values, respectively, for the data point i.

For the first time, three submillimeter-wave lines have been measured for the $H_2{}^{120}Te$ isotopomer containing the least abundant tellurium isotope with only 0.096% natural abundance. In predicting the transition frequencies for this molecule, we follow the method described by Edwards and co-workers (*20, 32*). We use a polynomial expansion in the tellurium mass difference to estimate the rotational constants in the vibrational ground state of $H_2{}^{120}Te$ and obtain A = 187548.62(2) MHz, B = 182757.335(4) MHz, and C = 91068.125(2) MHz. One standard error in units of last digit is given in parentheses. The centrifugal distortion parameters were taken to be the same as for $H_2{}^{122}Te$. The three lines available for $H_2{}^{120}Te$ were then fitted by variation of the two parameters A and c_{11} (Table 3).

IV. SUMMARY AND CONCLUSION

We report here an experimental study of the rotational spectrum of the H_2Te molecule, based on Fourier transform spectra recorded in the far infrared spectral region and submillimeter-wave spectra recorded with a millimeter-wave

TABLE 2

Far Infrared Rotational Transitions in the Vibrational Ground State of $H_2{}^{130}Te$

obs.	o.−c.	unc.	J'	K'_a	K'_c	J''	K''_a	K''_c	obs.	o.−c.	unc.	J'	K'_a	K'_c	J''	K''_a	K''_c
27.40601	−0.52	0.3	4	1	4	3	0	3	62.65851	−0.06	0.1	6	4	2	5	5	1
27.50784	−0.39	0.4	10	7	4	10	6	5	63.39586	−0.04	0.1	15	5	10	15	4	11
27.73923	−0.25	0.2	2	2	0	1	1	1		−0.04	0.1	15	6	10	15	5	11
27.79117	−0.35	0.2	8	5	4	8	4	5	63.71790	−0.02	0.1	10	0	10	9	1	9
27.84583	−0.15	0.1	3	2	2	2	1	1		−0.02	0.1	10	1	10	9	0	9
27.91347	−0.27	0.1	7	3	4	7	2	5	63.88077	−0.05	0.1	9	2	8	8	1	7
28.04073	0.02	0.8	6	3	4	6	2	5		−0.05	0.1	9	1	8	8	2	7
28.14246	−0.02	0.2	5	1	4	5	0	5	63.92623	−0.16	0.1	14	5	10	14	4	11
33.62438	−0.09	0.1	4	1	3	3	2	2		−0.16	0.1	14	4	10	14	3	11
33.88157	−0.03	0.1	9	4	5	9	3	6	64.01590	−0.15	0.1	5	5	0	4	4	1
34.06681	−0.50	0.4	8	4	5	8	3	6	64.01953	0.02	0.1	8	3	6	7	2	5
34.23017	−0.02	0.1	7	2	5	7	1	6	64.13683	−0.03	0.1	7	3	4	6	4	3
34.30831	−0.12	0.1	3	3	1	2	2	0	64.20430	−0.04	0.1	7	4	4	6	3	3
34.37434	−0.17	0.1	6	2	5	6	1	6	64.43596	0.01	0.1	13	4	10	13	3	11
	−0.12	0.1	6	1	5	6	0	6		0.01	0.1	13	3	10	13	2	11
39.42131	−0.07	0.1	12	6	6	12	5	7	64.82197	−0.03	0.1	4	2	2	3	1	3
39.42853	−0.06	0.1	12	7	6	12	6	7	64.92288	−0.07	0.1	12	2	10	12	1	11
40.19017	−0.11	0.1	9	3	6	9	2	7		−0.07	0.1	12	3	10	12	2	11
40.40069	−0.07	0.1	4	3	2	3	2	1	64.99994	−0.02	0.1	4	3	2	3	0	3
40.40420	−0.02	0.1	8	3	6	8	2	7	65.38534	−0.03	0.1	11	2	10	11	1	11
	0.03	0.1	8	2	6	8	1	7		−0.03	0.1	11	1	10	11	0	11
40.59677	−0.09	0.1	7	2	6	7	1	7	65.68911	−0.02	0.1	6	5	2	5	4	1
	−0.08	0.1	7	1	6	7	0	7	69.41531	0.02	0.1	8	6	3	7	7	0
45.34652	0.14	0.1	13	6	7	13	5	8	69.72189	−0.36	0.3	5	4	1	4	3	2
45.58211	−0.16	0.1	7	0	7	6	1	6	69.75127	0.01	0.1	11	1	11	10	0	10
	−0.16	0.1	7	1	7	6	0	6		0.01	0.1	11	0	11	10	1	10
45.68224	−0.17	0.2	12	6	7	12	5	8	69.83764	−0.05	0.1	15	5	11	15	4	12
45.75894	−0.32	0.2	6	2	5	5	1	4		−0.05	0.1	15	4	11	15	3	12
45.83878	−0.11	0.1	5	2	3	4	3	2	69.88250	−0.07	0.1	7	4	3	6	5	2
46.56075	−0.08	0.1	9	2	7	9	1	8	69.91002	−0.00	0.1	10	2	9	9	1	8
	−0.08	0.1	9	3	7	9	2	8		0.00	0.1	10	1	9	9	2	8
46.85792	−0.07	0.1	3	3	1	2	0	2	70.03742	−0.05	0.3	9	3	7	8	2	6
46.87427	−0.08	0.1	4	4	1	3	3	0		−0.00	0.1	9	2	7	8	3	6
51.10163	−0.03	0.1	5	3	2	4	4	1	70.16249	−0.02	0.1	8	3	5	7	4	4
51.22451	0.05	0.2	14	7	8	14	6	9	70.17330	0.23	0.1	8	4	5	7	3	4
51.80455	−0.06	0.1	7	1	6	6	2	5	70.43266	−0.03	0.1	14	4	11	14	3	12
52.36371	−0.04	0.1	11	4	8	11	3	9		−0.03	0.1	14	3	11	14	2	12
	−0.03	0.1	11	3	8	11	2	9	70.82276	−0.02	0.1	7	5	3	6	4	2
52.69973	−0.09	0.1	10	2	8	10	1	9	71.00587	−0.10	0.1	13	2	11	13	1	12
	−0.09	0.1	10	3	8	10	2	9		−0.10	0.1	13	3	11	13	2	12
53.01200	−0.09	0.1	9	1	8	9	0	9	71.55521	0.01	0.1	12	2	11	12	1	12
	−0.09	0.1	9	2	8	9	1	9		0.01	0.1	12	1	11	12	0	12
53.01616	−0.14	0.1	5	4	2	4	3	1	71.97887	−0.03	0.1	6	6	1	5	5	0
57.52972	−0.10	0.1	14	5	9	14	4	10	72.13268	0.06	0.1	5	5	1	4	2	2
	−0.12	0.1	14	6	9	14	5	10	73.94904	0.02	0.1	7	5	2	6	6	1
57.67816	−0.08	0.1	9	0	9	8	1	8	75.77766	0.03	0.1	12	1	12	11	0	11
	−0.08	0.1	9	1	9	8	0	8		0.03	0.1	12	0	12	11	1	11
57.84541	−0.07	0.1	8	2	7	7	1	6	75.93244	−0.00	0.1	11	2	10	10	1	9
	−0.06	0.1	8	1	7	7	2	6		−0.00	0.1	11	1	10	10	2	9
57.94048	−0.05	0.1	6	3	3	5	4	2	75.96027	−0.18	0.2	6	6	0	5	5	1
57.98202	0.01	0.1	13	5	9	13	4	10	76.04902	0.01	0.1	10	2	8	9	3	7
	0.01	0.1	13	4	9	13	3	10		0.01	0.1	10	3	8	9	2	7
57.99389	−0.20	0.2	7	2	5	6	3	4	76.16080	0.41	0.5	9	3	6	8	4	5
57.99710	0.13	0.2	7	3	5	6	2	4	76.22549	−0.00	0.1	8	4	4	7	5	3
58.40600	−0.04	0.1	6	4	3	5	3	2	76.39578	0.00	0.1	8	5	4	7	4	3
58.82064	−0.07	0.1	11	2	9	11	1	10	76.87141	0.00	0.1	5	3	2	4	2	3
	−0.07	0.1	11	3	9	11	2	10	77.06901	−0.12	0.1	14	2	12	14	1	13
59.20416	−0.03	0.1	10	2	9	10	1	10		−0.12	0.1	14	3	12	14	2	13
	−0.03	0.1	10	1	9	10	0	10	77.28377	0.02	0.1	5	4	2	4	1	3
59.44160	−0.04	0.1	5	5	1	4	4	0	77.71324	0.01	0.1	13	2	12	13	1	13
	0.01	0.1	13	1	12	13	0	13	99.80123	0.01	0.1	16	1	16	15	0	15
78.41351	−0.02	0.1	7	6	2	6	5	1		0.01	0.1	16	0	16	15	1	15
81.41588	0.02	0.1	6	5	1	5	4	2	99.94183	−0.05	0.1	15	1	14	14	2	13
81.60755	−0.18	0.1	8	5	3	7	6	2		−0.05	0.1	15	2	14	14	1	13
81.79643	0.01	0.1	13	1	13	12	0	12	99.99477	0.02	0.1	10	6	4	9	7	3
	0.01	0.1	13	0	13	12	1	12	100.01594	−0.03	0.1	14	2	12	13	3	11
81.94750	0.04	0.1	12	2	11	11	1	10		−0.03	0.1	14	3	12	13	2	11
	0.04	0.1	12	1	11	11	2	10	100.06064	−0.03	0.1	13	3	10	12	4	9
82.05335	0.02	0.1	11	3	9	10	2	8		−0.03	0.1	13	4	10	12	3	9
	0.02	0.1	11	2	9	10	3	8	100.10752	−0.09	0.2	12	5	8	11	4	7
82.14829	0.07	0.2	10	4	7	9	3	6	100.19586	−0.09	0.1	11	6	6	10	5	5
	0.30	0.5	10	3	7	9	4	6	100.43648	0.21	0.1	7	5	2	6	4	3
82.25048	0.00	0.1	9	4	5	8	5	4	100.75083	−0.10	0.1	10	7	4	9	6	3
82.28210	−0.06	0.1	9	5	5	8	4	4	101.88880	−0.06	0.1	7	6	2	6	3	3
83.11167	−0.11	0.1	15	2	13	15	1	14	101.94241	−0.03	0.9	6	3	4	5	0	5
	−0.11	0.1	15	3	13	15	2	14	103.96830	−0.02	0.1	9	8	2	8	7	1
83.30933	0.01	0.1	8	6	3	7	5	2	104.12502	−0.09	0.1	10	7	3	9	8	2
83.43236	0.05	0.1	5	2	3	4	1	4	104.38235	−0.03	0.1	8	7	1	7	6	2
83.85900	−0.02	0.1	14	1	13	14	0	14	105.78353	−0.07	0.1	17	1	17	16	0	16
	−0.02	0.1	14	2	13	14	1	14		−0.07	0.1	17	0	17	16	1	16

Note: Observed transition wavenumbers are given in cm^{-1}. Residuals (observed — calculated) and uncertainties are given in $cm^{-1} \times 10^{-3}$.

TABLE 2—*Continued*

obs.	o.-c	unc.	J'	K'_a	K'_c	J''	K''_a	K''_c	obs.	o.-c.	unc.	J'	K'_a	K'_c	J''	K''_a	K''_c
84.45263	−0.02	0.1	7	7	1	6	6	0	105.92100	−0.08	0.1	16	1	15	15	2	14
84.89331	0.02	0.1	6	6	1	5	3	2		−0.08	0.1	16	2	15	15	1	14
84.95057	−0.04	0.1	8	6	2	7	7	1	105.98446	−0.07	0.1	15	2	13	14	3	12
87.80709	0.07	0.1	14	0	14	13	1	13		−0.07	0.1	15	3	13	14	2	12
	0.07	0.1	14	1	14	13	0	13	106.01257	−0.13	0.1	14	3	11	13	4	10
87.84312	0.07	0.1	7	7	0	6	6	1		−0.13	0.1	14	4	11	13	3	10
87.95453	0.08	0.1	13	1	12	12	2	11	106.03753	0.02	0.1	13	5	9	12	4	8
	0.08	0.1	13	2	12	12	1	11		0.05	0.1	13	4	9	12	5	8
88.04995	0.25	0.3	12	2	10	11	3	9	106.07551	0.26	0.3	10	8	2	9	9	1
	0.25	0.3	12	3	10	11	2	9	106.08721	−0.07	0.1	12	5	7	11	6	6
88.12747	−0.12	0.1	11	3	8	10	4	7	106.09031	−0.09	0.1	12	6	7	11	5	6
88.19149	−0.05	0.1	9	5	4	8	6	3	106.11466	0.22	0.2	11	6	5	10	7	4
88.21791	0.00	0.1	10	4	6	9	5	5	106.30535	−0.04	0.1	11	7	5	10	6	4
88.22286	−0.03	0.1	10	5	6	9	4	5	107.47659	−0.05	0.1	7	4	3	6	3	4
88.56870	0.01	0.1	9	6	4	8	5	3	107.62192	−0.10	0.1	7	5	3	6	2	4
88.75539	−0.01	0.1	6	4	2	5	3	3	108.55692	−0.07	0.1	10	8	3	9	7	2
89.57258	0.09	0.1	6	5	2	5	2	3	109.08761	−0.04	0.1	9	9	1	8	8	0
89.99204	−0.04	0.1	15	2	14	15	1	15	110.72509	0.02	0.1	8	8	1	7	5	2
	−0.04	0.1	15	1	14	15	0	15	111.43199	−0.04	0.1	9	9	0	8	8	1
91.17906	−0.09	0.1	8	7	2	7	6	1	111.58272	−0.09	0.1	11	7	4	10	8	3
92.96816	−0.05	0.1	7	6	1	6	5	2	111.75531	−0.04	0.1	18	1	18	17	0	17
93.80880	−0.02	0.1	15	1	15	14	0	14		−0.04	0.1	18	0	18	17	1	17
	−0.02	0.1	15	0	15	14	1	14	111.88971	−0.06	0.1	17	1	16	16	2	15
93.95281	0.01	0.1	14	1	13	13	2	12		−0.06	0.1	17	2	16	16	1	15
	0.01	0.1	14	2	13	13	1	12	111.94242	−0.09	0.1	16	2	14	15	3	13
94.03746	−0.01	0.1	13	2	11	12	3	10		−0.09	0.1	16	3	14	15	2	13
	−0.01	0.1	13	3	11	12	2	10	112.03796	−0.13	0.1	12	6	6	11	7	5
94.09868	−0.03	0.1	12	3	9	11	4	8	112.07739	−0.02	0.1	12	7	6	11	6	5
	−0.04	0.1	12	4	9	11	3	8	112.98222	0.03	0.1	11	8	4	10	7	3
94.16773	0.10	0.3	11	4	7	10	5	6	113.94848	−0.06	0.1	7	3	4	6	2	5
94.32370	−0.15	0.2	10	6	5	9	5	4	113.95800	0.06	0.1	7	4	4	6	1	5
95.51221	−0.08	0.1	6	3	3	5	2	4	114.26477	−0.03	0.1	8	7	2	7	4	3
95.57087	−0.08	0.1	6	4	3	5	1	4	114.75770	−0.05	0.1	11	8	3	10	9	2
95.65613	0.00	0.1	9	7	2	8	8	1	115.67138	−0.09	0.1	9	8	1	8	7	2
95.88429	−0.03	0.1	9	7	3	8	6	2	116.23386	−0.13	0.1	11	9	2	10	10	1
96.11202	0.09	0.1	16	2	15	16	1	16	116.75358	−0.11	0.1	10	9	2	9	8	1
	0.09	0.1	16	1	15	16	0	16	117.71586	−0.02	0.1	19	1	19	18	0	18
96.83083	−0.21	0.1	8	8	1	7	7	0		−0.02	0.1	19	0	19	18	1	18
97.75454	0.01	0.1	7	7	1	6	4	2	117.83940	0.02	0.1	12	7	5	11	8	4
99.66731	−0.05	0.1	8	8	0	7	7	1	117.84738	0.04	0.1	18	2	17	17	1	16
	0.04	0.1	18	1	17	17	2	16	135.51496	0.03	0.1	18	5	14	17	4	13
117.86151	−0.30	0.2	14	6	9	13	5	8		0.03	0.1	18	4	14	17	5	13
117.86529	−0.11	0.1	15	4	11	14	5	10	135.52392	−0.07	0.1	22	1	22	21	0	21
	−0.11	0.1	15	5	11	14	4	10		−0.07	0.1	22	0	22	21	1	21
117.88405	−0.10	0.1	16	3	13	15	4	12	135.57992	−0.08	0.3	14	9	6	13	8	5
	−0.10	0.3	16	4	13	15	3	12	135.64740	0.05	0.1	21	2	20	20	1	19
117.88945	0.21	0.3	17	2	15	16	3	14		0.05	0.1	21	1	20	20	2	19
	0.21	0.1	17	3	15	16	2	14	135.65551	0.01	0.1	20	2	18	19	3	17
117.89784	−0.14	0.1	13	6	7	12	7	6		0.01	0.1	20	3	18	19	2	17
117.90730	0.13	0.1	13	7	7	12	6	6	136.98029	0.02	0.1	10	10	1	9	7	2
118.24516	−0.06	0.1	12	8	5	11	7	4	137.62722	0.03	0.1	9	5	4	8	4	5
119.29222	−0.02	0.1	8	5	3	7	4	4	137.69837	−0.06	0.1	9	6	4	8	3	5
119.60868	−0.04	0.1	8	6	3	7	3	4	137.78133	−0.05	0.1	13	10	4	12	9	3
120.40935	0.04	0.2	7	2	5	6	1	6	137.97956	−0.05	0.1	11	10	1	10	9	2
121.20430	−0.06	0.1	10	10	1	9	9	0	138.84661	0.06	0.1	8	3	6	7	0	7
121.32315	−0.03	0.1	11	9	3	10	8	2	139.37726	−0.08	0.1	10	9	2	9	6	3
122.88977	−0.10	0.1	12	8	4	11	9	3	141.15297	−0.16	0.5	15	8	7	14	9	6
123.07186	−0.01	0.1	9	7	2	8	6	3	141.26179	0.00	0.1	18	6	13	17	5	12
123.66459	0.02	0.1	20	0	20	19	1	19		0.00	0.1	18	5	13	17	6	12
	0.02	0.1	20	1	20	19	0	19	142.15430	−0.06	0.1	12	11	2	11	10	1
123.73154	0.07	0.2	15	5	10	14	6	9	142.29929	−0.09	0.1	10	7	3	9	6	4
123.73982	−0.07	0.2	14	7	8	13	6	7	143.43729	−0.03	0.1	10	8	3	9	5	4
123.76130	−0.39	0.3	16	4	12	15	5	11	144.10929	−0.01	0.1	9	4	5	8	3	6
	−0.39	0.3	16	5	12	15	4	11	144.11349	−0.03	0.1	9	5	5	8	2	6
123.77442	0.09	0.1	13	7	6	12	8	5	144.65727	0.01	0.1	11	9	2	10	8	3
123.79308	−0.11	0.1	19	2	18	18	1	17	144.99173	−0.04	0.1	12	12	1	11	11	0
	−0.11	0.1	19	1	18	18	2	17	146.30673	−0.02	0.1	12	12	0	11	11	1
123.82398	−0.10	0.1	18	3	16	17	2	15	149.25380	0.02	0.1	10	6	4	9	5	5
	−0.10	0.1	18	2	16	17	3	15	149.41728	0.00	0.1	10	7	4	9	4	5
123.86881	−0.03	0.1	13	8	6	12	7	5	150.22878	0.09	0.1	11	11	1	10	8	2
124.86934	−0.12	0.1	12	9	3	11	10	2	150.63169	−0.22	0.2	9	3	6	8	2	7
125.31011	0.01	0.1	12	9	4	11	8	3	152.23203	0.03	0.1	11	10	2	10	7	3
125.85044	−0.09	0.1	8	4	4	7	3	5	154.67722	−0.15	0.1	13	12	2	12	11	1
125.87835	0.02	0.1	8	5	4	7	2	5	155.07762	−0.06	0.1	12	10	2	11	9	3
126.74291	−0.06	0.1	9	8	2	8	5	3	155.32385	0.11	0.1	11	9	3	10	6	4
126.85961	0.04	0.1	10	9	1	9	8	2	155.77779	−0.43	0.4	10	5	5	9	4	6
129.37509	−0.07	0.1	13	8	5	12	9	4	155.79060	−0.04	0.1	10	6	5	9	3	6
129.49749	−0.06	0.1	11	10	2	10	9	1	156.67029	−0.07	0.1	13	13	1	12	12	0
129.56421	0.10	0.2	15	6	9	14	7	8	157.25116	−0.00	0.1	9	3	7	8	0	8
129.60092	0.12	0.1	21	0	21	20	1	20		0.00	0.1	9	2	7	8	1	8
	0.12	0.1	21	1	21	20	0	20	157.77366	0.07	0.1	13	13	0	12	12	1
129.61496	0.18	0.1	14	8	7	13	7	6	159.87226	−0.08	0.1	14	12	3	13	11	2
129.70739	0.06	0.1	18	4	15	17	3	14	160.69629	0.00	0.1	11	7	4	10	6	5
	0.06	0.1	18	3	15	17	4	14	161.03992	−0.03	0.1	11	8	4	10	5	5

TABLE 2—*Continued*

obs.	o−c.	unc.	J'	K'_a	K'_c	J''	K''_a	K''_c	obs	o.−c.	unc.	J'	K'_a	K'_c	J''	K''_a	K''_c
129.72667	−0.05	0.1	20	2	19	19	1	18	162.29457	−0.19	0.3	10	5	6	9	2	7
	−0.05	0.1	20	1	19	19	2	18	164.11906	−0.22	0.1	12	9	3	11	8	4
129.74627	−0.10	0.1	19	2	17	18	3	16	165.29273	0.08	0.3	13	11	2	12	10	3
	−0.10	0.1	19	3	17	18	2	16	165.37628	0.05	0.1	12	11	2	11	8	3
130.91675	−0.07	0.1	9	6	3	8	5	4	167.02789	0.14	0.1	14	13	2	13	12	1
131.54116	−0.03	0.1	9	7	3	8	4	4	167.23646	−0.05	0.1	12	10	3	11	7	4
132.31685	−0.16	0.4	8	4	5	7	1	6	167.30892	0.09	0.1	11	6	5	10	5	6
133.17232	−0.07	0.1	11	11	1	10	10	0	167.34139	0.13	0.1	11	7	5	10	4	6
133.83750	−0.06	0.1	13	9	4	12	10	3	168.22330	0.07	0.1	14	14	1	13	13	0
133.99526	−0.07	0.1	10	8	2	9	7	3	168.89937	0.05	0.1	10	4	7	9	1	8
134.16198	−0.07	0.1	12	10	3	11	9	2		0.08	0.1	10	3	7	9	2	8
134.75853	−0.03	0.1	11	11	0	10	10	1	169.16249	0.16	0.1	14	14	0	13	13	1
135.37342	−0.11	0.1	15	7	8	14	8	7	171.90817	−0.06	0.1	12	8	4	11	7	5
135.37727	0.02	0.2	16	7	10	15	6	9	172.57981	−0.01	0.1	12	9	4	11	6	5
135.43241	0.03	0.1	17	6	12	16	5	11	173.82348	−0.04	0.1	11	5	6	10	4	7
	0.03	0.1	17	5	12	16	6	11	174.46870	−0.01	0.1	13	10	3	12	9	4
175.62195	0.02	0.1	10	3	8	9	0	9	198.46771	0.05	0.1	12	5	8	11	2	9
	0.02	0.1	10	2	8	9	1	9		0.08	0.1	12	4	8	11	3	9
178.68321	−0.18	0.1	12	7	5	11	6	6	203.00875	−0.22	0.1	13	6	7	12	5	8
178.76049	0.08	0.1	12	8	5	11	5	6	205.28330	0.12	0.1	12	4	9	11	1	10
180.41342	0.03	0.2	11	4	7	10	3	8		0.12	0.1	12	3	9	11	2	10
180.48323	0.03	0.1	15	15	0	14	14	1	209.66771	−0.07	0.1	13	5	8	12	4	9
182.36838	−0.17	0.1	15	14	1	14	13	2	212.25586	0.08	0.1	12	3	10	11	0	11
182.82883	−0.01	0.1	13	9	4	12	8	5		0.08	0.1	12	2	10	11	1	11
185.21859	−0.00	0.1	12	7	6	11	4	7	216.45551	0.07	0.1	13	5	9	12	2	10
187.11696	0.06	0.1	11	4	8	10	1	9		0.07	0.1	13	4	9	12	3	10
	0.07	0.1	11	3	8	10	2	9	220.71110	−0.28	0.2	14	7	8	13	4	9
189.87761	0.04	0.1	13	8	5	12	7	6	223.39653	0.15	0.1	13	4	10	12	1	11
191.04453	−0.25	0.1	16	16	1	15	15	0		0.15	0.1	13	3	10	12	2	11
191.78615	−0.18	0.2	12	6	7	11	3	8	227.46878	−0.15	0.1	14	6	9	13	3	10
193.95745	0.11	0.1	11	3	9	10	0	10		−0.12	0.1	14	5	9	13	4	10
	0.11	0.1	11	2	9	10	1	10	234.37520	0.16	0.1	14	5	10	13	2	11
196.44437	0.01	0.1	13	7	6	12	6	7		0.16	0.1	14	4	10	13	3	11

spectrometer or a laser sideband system. We have assigned 1695 far infrared lines and 224 submillimeter-wave lines, thus greatly extending the number of spectroscopic data available for the vibrational ground state of H_2Te. The data were fitted separately for each isotopomer and accurate sets of rotational and centrifugal distortion parameters were obtained for eight H_2Te isotopomers (containing eight Te isotopes in natural abundance).

As described above, we have used the modified Watson Hamiltonian of Eq. [1] to fit data sets of rotational transition frequencies/wavenumbers for the isotopomers of H_2Te. We have also made these fits using a standard Watson Hamiltonian in A reduction and I^r representation. However with this Hamiltonian, the parameters obtained exhibit very strong correlations. Watson *et al.* (*33*) discuss how the diagonal elements of the inverse correlation matrix measure the ''cumulative'' correlation of a given parameter with all other parameters. For the standard Watson Hamiltonian, these diagonal elements attained values up to 10^7 in a 35-parameter fit to the data of $H_2{}^{130}Te$. With the modified Hamiltonian of Eq. [1], the largest diagonal elements of the inverse correlation matrix were smaller by two orders of magnitude relative to the values obtained with the standard effective Hamiltonian. Owing to the very strong correlation of the ''standard Watsonian'' parameters, we could not reproduce the experimental submillimeter-wave data using parameters values rounded off after the third digit of the standard error. Such problems are well known and have been discussed, for example, by Watson (*34*) and by Tellinghuisen (*35*). The parameters of the modified Watson Hamiltonian (Eq. [1]) appear to be less correlated. However, when we round off the parameter values of the modified Hamiltonian after the second digit of the standard error, we still cannot reproduce the experimental submillimeter-wave data. Therefore, we provide in Table 3 parameter values rounded off after the third digit of the standard error, and these values produce the residuals given in Tables 1 and 2. The modification of the Watson Hamiltonian has been made in a purely empirical manner. By means of semiclassical theory, it can be argued (*36*) that the modified Hamiltonian is more suitable for some molecules than the standard Watson form. However, the problem of high correlations in effective Hamiltonians and the choice of appropriate parameter sets require a separate theoretical study.

Generally all the data were fitted well. For example, the dimensionless standard deviations for the far infrared lines indicate that residuals of the fitting are very close to the wavenumber uncertainty estimated from the calibration procedure. An exception is $H_2{}^{125}Te$, which has a dimensionless submillimeter-wave standard deviation of 1.35. This, however, reflects the quality of the input data rather than that of the model used. We believe that the fitting for this isotopomer can be usefully improved only by excluding some earlier measured submillimeter-wave lines.

TABLE 3

Rotational and Centrifugal Distortion Constants of H_2Te in the Vibrational Ground State

	$H_2{}^{130}Te$	$H_2{}^{128}Te$	$H_2{}^{126}Te$	$H_2{}^{125}Te$	$H_2{}^{124}Te$	$H_2{}^{123}Te$	$H_2{}^{122}Te$	$H_2{}^{120}Te$
A/GHz	187.31046759(743)	187.35520958(810)	187.40133662(956)	187.4248625(114)	187.4489622(123)	187.4732411(362)	187.4980912(141)	187.549067(11)
B/GHz	182.75703361(723)	182.75711872(864)	182.75715967(959)	182.7571843(107)	182.7572189(120)	182.7571639(277)	182.7572909(180)	182.757335(4)[c]
C/GHz	91.01147173(519)	91.02211734(564)	91.03308520(585)	91.03867044(610)	91.04441135(645)	91.0502109(104)	91.05609589(820)	91.068125(2)[c]
c_{20}/MHz	−11.110687(159)	−11.111621(237)	−11.111108(304)	−11.110256(291)	−11.110438(348)	−11.113739(995)	−11.110831(650)	−11.110831[d]
c_{11}/MHz	17.908224(439)	17.909146(693)	17.911388(849)	17.916517(861)	17.91413(103)	17.92028(377)	17.91626(183)	17.85696(23)
c_{02}/MHz	−24.662552(301)	−24.675679(381)	−24.688612(548)	−24.695041(717)	−24.702945(809)	−24.70017(258)	−24.714537(902)	−24.714537[d]
b_{10}/MHz	−5.1614987(707)	−5.161661(106)	−5.161432(140)	−5.161341(141)	−5.161312(174)	−5.160230(581)	−5.161314(311)	−5.161314[d]
b_{01}/MHz	−0.358129(134)	−0.362553(189)	−0.366139(245)	−0.368228(265)	−0.369196(301)	−0.375794(920)	−0.373450(462)	−0.373450[d]
c_{30}/kHz	4.09433(174)	4.10289(275)	4.09239(483)	4.09416(456)	4.08312(548)	4.1732(163)	4.0886(103)	4.0886[d]
c_{21}/kHz	−11.61328(607)	−11.5783(107)	−11.5685(170)	−11.6676(156)	−11.6074(180)	−11.6717(485)	−11.5748(344)	−11.5748[d]
c_{12}/kHz	−9.15909(986)	−9.1814(171)	−9.1814(260)	−9.2247(218)	−9.1561(249)	−9.384(106)	−9.2047(444)	−9.2047[d]
c_{03}/kHz	11.02334(424)	11.04756(531)	11.07918(993)	11.1203(157)	11.1392(176)	10.9005(432)	11.0945(131)	11.0945[d]
b_{20}/kHz	2.041494(889)	2.04404(139)	2.03986(246)	2.04246(233)	2.03668(284)	2.06181(822)	2.03947(532)	2.03947[d]
b_{11}/kHz	−3.90543(256)	−3.89449(464)	−3.89309(723)	−3.91977(549)	−3.90584(654)	−3.9220(171)	−3.9202(116)	−3.9202[d]
b_{02}/kHz	7.84159(420)	7.87705(655)	7.88384(949)	7.89922(990)	7.8467(110)	8.0732(536)	7.8777(189)	7.8777[d]
c_{40}/Hz	−2.30471(915)	−2.3405(134)	−2.2844(376)	−2.3331(248)	−2.2478(290)	−2.835(118)	−2.2968(573)	−2.2968[d]
c_{31}/Hz	10.0732(624)	9.842(126)	9.819(237)	10.469(105)	10.137(123)	11.033(345)	10.330(217)	10.330[d]
c_{22}/Hz	−5.3264(760)	−5.604(146)	−5.734(250)	−5.538(146)	−5.360(177)	−5.360[b]	−6.718(484)	−6.718[d]
c_{13}/Hz	11.1636(903)	11.679(178)	11.486(311)	11.680(184)	10.628(212)	14.58(108)	11.964(418)	11.964[d]
c_{04}/Hz	−7.0806(246)	−7.1703(285)	−7.3810(741)	−7.926(144)	−7.917(162)	−6.763(229)	−7.3451(685)	−7.3451[d]
b_{30}/Hz	−1.15449(471)	−1.16712(685)	−1.1441(190)	−1.1698(125)	−1.1278(147)	−1.3835(594)	−1.1534(291)	−1.1534[d]
b_{21}/Hz	3.6351(335)	3.5063(656)	3.557(117)	3.7587(515)	3.7653(658)	3.7653[b]	3.843(125)	3.843[d]
b_{12}/Hz	0.0	0.0	0.0	0.0	0.0	0.0	0.0	0.0
b_{03}/Hz	−10.7167(460)	−11.1288(758)	−11.235(126)	−11.0538(905)	−10.5530(999)	−13.054(735)	−10.826(195)	−10.826[d]
c_{50}/mHz	1.1792(196)	1.2258(273)	1.186(109)	1.1792[a]	1.1792[a]	1.1792[a]	1.1792[a]	1.1792[a]
c_{41}/mHz	−6.193(209)	−5.369(484)	−5.939(934)	−6.193[a]	−6.193[a]	−6.193[a]	−6.193[a]	−6.193[a]
c_{32}/mHz	0.0	0.0	0.0	0.0	0.0	0.0	0.0	0.0
c_{23}/mHz	7.859(454)	9.22(103)	12.81(222)	7.859[a]	7.859[a]	7.859[a]	7.859[a]	7.859[a]
c_{14}/mHz	−11.038(320)	−13.806(758)	−15.14(124)	−11.038[a]	−11.038[a]	−11.038[a]	−11.038[a]	−11.038[a]
c_{05}/mHz	3.7720(506)	3.9224(564)	4.608(197)	6.487(472)	6.258(526)	6.258[b]	3.7720[a]	3.7720[a]
b_{40}/mHz	0.59623(993)	0.6148(138)	0.6022(549)	0.59623[a]	0.59623[a]	0.59623	0.59623[a]	0.59623[a]
b_{31}/mHz	−2.257(107)	−1.883(238)	−2.202(450)	−2.257[a]	−2.257[a]	−2.257[a]	−2.257[a]	−2.257[a]
b_{22}/mHz	2.150(113)	2.990(215)	2.541(477)	2.150[a]	2.150[a]	2.150[a]	2.150[a]	2.150[a]
b_{13}/mHz	−2.930(110)	−3.887(270)	−2.462(482)	−2.930[a]	−2.930[a]	−2.930[a]	−2.930[a]	−2.930[a]
b_{04}/mHz	10.368(150)	12.088(278)	12.351(502)	10.368[a]	10.368[a]	10.368[a]	10.368[a]	10.368[a]
Submm St.D.	0.92	0.88	1.05	1.35	1.05	0.46	0.68	0.34
FIR St.D.	0.70	0.71	0.84	0.71	0.86	0.72	0.84	
GSCD St.D.	0.53	0.54	0.51	0.58	0.59	0.64	0.74	
Number of Submm lines	86	86	33	33	32	18	27	3
Number of FIR lines	394	381	343	201	172	59	145	
Number of GSCD's	8446	3396	3092	2131	1817	161	1178	

[a] Constrained to the value for $H_2{}^{130}Te$. [b] Constrained to the value for $H_2{}^{124}Te$. [c] Determined from polynomial extrapolation (see text). [d] Constrained to the value for $H_2{}^{122}Te$.

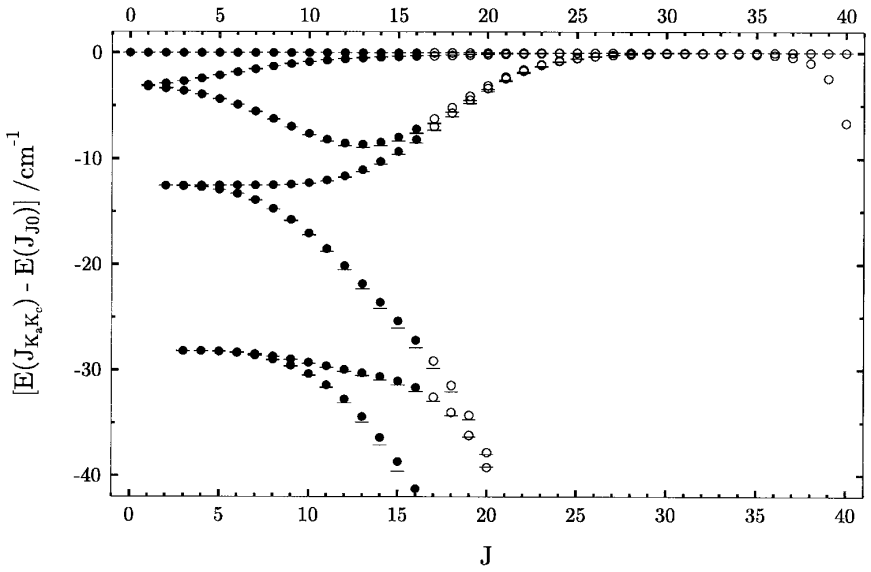

FIG. 2. The rotational energy level structure of the ground vibrational state of $H_2{}^{130}Te$. Term values are plotted relative to the highest term value in each J multiplet. Filled circles show term values derived from the spectra analyzed in the present work; empty circles show extrapolated term values obtained from the effective Hamiltonian of Eq. [1] with the parameter values from Table 3; and horizontal lines indicate term values predicted with the MORBID program (*16*).

In Fig. 2 we compare the rotational term values obtained in the present work with predictions calculated with the MORBID Hamiltonian and computer program (*1, 16*) from a potential energy surface obtained in a least-squares fit (using the MORBID program) to experimental term values involving $J \leqslant 5$ from Refs. (*17–23*). We use $H_2{}^{130}Te$ as example since for this isotopomer, the largest set of experimentally derived term values is available. Although transitions involving $J \leqslant 22$ have been measured, it turned out to be very difficult to observe transitions to the top levels in the J multiplet ($K_a \approx J$), for which the cluster effect occurs. The cluster formation starts at $J = J_c$, the critical J value (see above), which is predicted to be between 8 and 10 (depending on the model used) for $H_2{}^{130}Te$. Figure 2 shows that in reality, the energy difference between the highest two doublets in the J manifolds starts decreasing with J at slightly higher $J \approx 14$. The experimentally derived term values for the cluster states extend up to $J = K_a = 16$. Hence, we have experimental proof that the energy difference between the two highest energy doublets decreases with J, but with the available experimental data we are still far from the situation of near-degenerate doublets. Obviously the necessity of cooling the H_2Te sample strongly reduces our ability to observe transitions to highly excited rotational levels.

Figure 2 contains an extrapolation to the term values for higher J values using the Hamiltonian of Eq. [1] with the parameters of Table 3. It is seen that the MORBID prediction agrees remarkably well with the experimentally derived term values and with the values predicted from the Watson-type Hamiltonian at moderate J values, but that the effective Hamiltonian becomes divergent when J increases further.

The present work has essentially extended the amount of experimental rotational data available for the vibrational ground state of the H_2Te molecule. We hope to use the new data, together with the rotation–vibration data determined in Refs. (*24, 25*), to refine the potential energy surface for H_2Te in a least-squares fit using the MORBID program.

The experimental data obtained in the present work confirm the conclusion of previous theoretical calculations (*1, 15*): The rotational energy level structure of the ground vibrational state of H_2Te is very similar to that of H_2Se (*2, 4*). However, in spite of the fact that we have measured H_2Te transitions to rotational states with J values above the critical value J_c, the J values attained are still not sufficiently high for nearly degenerate clusters to be observed. Further experimental work in this direction is required.

ACKNOWLEDGMENTS

We are very grateful to H. Bürger, J.-M. Flaud, B. P. Winnewisser, and M. Winnewisser for their encouragement and advice. The help of G. Ch. Mellau in the data processing at Giessen is gratefully acknowledged. This work was supported in part by the Deutsche Forschungsgemeinschaft (through Forschergruppe Grants Bu 152/12-4 and Bu 152/12-

5), by the European Commission through Contract CHRX-CT94-0665, ''Highly Excited Rovibrational States,'' and by the Fonds der Chemischen Industrie. I. N. K. is grateful to the German Academic Exchange Service (DAAD) for a fellowship and to the Russian Fund for Fundamental Investigation Grant 94-02-05424-a for support.

REFERENCES

1. P. Jensen, G. Osmann, and I. N. Kozin, *in* ''Advanced Series in Physical Chemistry: Vibration–Rotational Spectroscopy and Molecular Dynamics'' (D. Papoušek, Ed.). World Scientific, Singapore, in press.
2. I. N. Kozin, S. P. Belov, O. L. Polyansky, and M. Yu. Tretyakov, *J. Mol. Spectrosc.* **152,** 13 (1992).
3. I. N. Kozin, O. L. Polyansky, S. I. Pripolzin, and V. L. Vaks, *J. Mol. Spectrosc.* **156,** 504 (1993).
4. I. N. Kozin, S. Klee, P. Jensen, O. L. Polyansky, and I. M. Pavlichenkov, *J. Mol. Spectrosc.* **158,** 409 (1993).
5. J.-M. Flaud, C. Camy-Peyret, H. Bürger, P. Jensen, and I. N. Kozin, *J. Mol. Spectrosc.* **172,** 126 (1995).
6. B. I. Zhilinskii and I. M. Pavlichenkov, *Opt. Spectrosk.* **64,** 413 (1988).
7. I. M. Pavlichenkov and B. I. Zhilinskii, *Ann. Phys. (N. Y.)* **184,** 1 (1988).
8. I. M. Pavlichenkov, *Phys. Rep.* **226,** 175 (1993).
9. J. Makarewicz and J. Pyka, *Mol. Phys.* **69,** 107 (1989).
10. P. Jensen, *J. Mol. Spectrosc.* **128,** 478 (1988).
11. P. Jensen, *J. Chem. Soc. Faraday Trans. 2* **84,** 1315 (1988).
12. I. N. Kozin and P. Jensen, *J. Mol. Spectrosc.* **163,** 483 (1994).
13. P. Jensen and I. N. Kozin, *J. Mol. Spectrosc.* **160,** 39 (1993).
14. I. N. Kozin and P. Jensen, *J. Mol. Spectrosc.* **161,** 186 (1993).
15. P. Jensen, Y. Li, G. Hirsch, R. J. Buenker, T. J. Lee, and I. N. Kozin, *Chem. Phys.* **190,** 179 (1995).
16. G. Osmann, M. Sc. Thesis, University of Wuppertal, 1994.
17. K. Rossmann and J. W. Straley, *J. Chem. Phys.* **24,** 1276 (1956).
18. R. A. Hill, T. H. Edwards, K. Rossmann, K. Narahari Rao, and H. H. Nielsen, *J. Mol. Spectrosc.* **14,** 221 (1964).
19. N. K. Moncur and T. H. Edwards, *J. Chem. Phys.* **51,** 2638 (1969).
20. N. K. Moncur, P. D. Willson, and T. H. Edwards, *J. Mol. Spectrosc.* **52,** 181 (1974).
21. P. D. Willson, N. K. Moncur, and T. H. Edwards, *J. Mol. Spectrosc.* **52,** 196 (1974).
22. N. K. Moncur, P. D. Willson, and T. H. Edwards, *J. Mol. Spectrosc.* **52,** 380 (1974).
23. A. V. Burenin, A. F. Krupnov, S. V. Mart'yanov, A. A. Mel'nikov, and L. I. Nikolayev, *J. Mol. Spectrosc.* **75,** 333 (1979).
24. H. Bürger, J.-M. Flaud, L. Halonen, and O. Polanz, in preparation.
25. J.-M. Flaud, M. Betrencourt, Ph. Arcas, H. Bürger, O. Polanz, and W. J. Lafferty, submitted for publication.
26. G. Brauer, ''Handbuch der Präparativen Anorganischen Chemie.'' Ferdinand Enke Verlag, Stuttgart, 1975.
27. I. M. Mills, T. Cvitaš, K. Homann, N. Kallay, and K. Kuchitsu, ''Quantities, Units and Symbols in Physical Chemistry.'' Blackwell, London, 1993.
28. R. Schermaul, J. W. G. Seibert, G. Ch. Mellau, and M. Winnewisser, *Appl. Opt.* **35,** 2884 (1996).
29. I. N. Kozin, P. Jensen, Y. Li, R. J. Buenker, G. Hirsch, and S. Klee, *J. Mol. Spectrosc.*, in press.
30. G. Guelachvili and K. Narahari Rao, ''Handbook of Infrared Standards.'' Academic Press, Orlando, FL, 1986.
31. D. Boucher, R. Bocquet, J. Burie, and W. Chen, *J. Phys. III (France)* **4,** 1467 (1994).
32. Wm. C. Lane, T. H. Edwards, J. R. Gillis, F. S. Bonomo, and F. J. Murcray, *J. Mol. Spectrosc.* **107,** 306 (1984).
33. J. K. G. Watson, S. C. Foster, A. R. W. McKellar, P. Bernath, T. Amano, F. S. Pan, M. W. Crofton, R. S. Altman, and T. Oka, *Can. J. Phys.* **62,** 1875 (1984).
34. J. K. G. Watson, *J. Mol. Spectrosc.* **66,** 500 (1977).
35. J. Tellinghuisen, *J. Mol. Spectrosc.* **137,** 248 (1989).
36. I. N. Kozin, Ph.D. Thesis, Nizhnii Novgorod (1995).